Safe nonlinear controller switching with biomedical engineering applications

Sung H. Cha, Arvin Dehghani and Brian D. O. Anderson

Abstract— **Suppose an unknown or only partially identified plant is operating with a known linear controller in a closed-loop, and the use of a known nonlinear controller appears attractive to replace the existing controller, on the basis of limited knowledge of the plant. We apply our novel data-based verification tests for ensuring that the introduction of the new nonlinear controller will stabilize the true plant for two different practical scenarios. First, we explore a dynamic mass system to illustrate how our tests can be utilized for verifying a nonlinear regulator given as a state feedback law. Second, we apply our tests to a biomedical engineering control problem in a multiple model adaptive control setting, where a nonlinear blood pressure regulator is required for better performance.**

I. Introduction

Suppose an unknown or partially known system is working with a stabilizing controller in a standard feedback setting. To account for unknownness, an adaptive control scheme may be used to secure satisfactory operation. An adaptive algorithm sometimes necessitates—often requires—switching from the entire or at least part of the current controller to a new controller after a certain period of time [1]. Such switching algorithms depend on collection of the available closed-loop signals and analysis before switching. Since these signals may be noisy, they may be inadequate to correctly determine the replacement controller. Some schemes may even lead to connecting of a destabilizing controller, see e.g. [1], [2], [3]. Thus it is vital to develop some tests for verifying the stability of the closed-loop with the new controller before its actual insertion into the loop.

For the case of linear time-invariant (LTI) plant and controllers, there exist such data-based validation tests [4] for verifying that the introduction of a new controller will stabilize an unknown plant, originally in a standard feedback interconnection with a stabilizing controller. However, due to the limited analysis tools for nonlinear systems, it is not straightforward to readily develop such analogue tests, where any of the plant, old or new controllers are nonlinear.

We have devised analysis tools for the nonlinear feedback configuration of our interest by adopting a special representation of dynamic systems, called a 'kernel representation' from [5]. Building on these analysis results, we advance a novel data-based online test for verifying that the introduction of a new known *nonlinear* controller will stabilize an unknown LTI plant [6]. Our test requires only a limited amount of noisy input-output experimental data obtained from the stable closed-loop.

This manuscript focuses on applying our novel test in practical control engineering problems through two particular numerical case studies. First, we will consider a simple dynamic mass system given in [7], where a nonlinear state feedback regulator is as designed for over 40% reduction in both the rise time and settling time with zero % overshoot compared to its linear counterpart. As the nonlinear controller is given as a state feedback law, we will also discuss how to implement such designs for the purpose of our nonlinear controller verification. Second, we will adopt a more practical example of a blood pressure control given in [8], where a multiple-model adaptive control (MMAC) design is used for sodium nitroprusside (SNP) regulation of arterial pressure. Since MMAC algorithm normally utilizes several local controllers during its operation, our data-based stability verification test ensures safety in this biomedical engineering application.

The structure of the paper is as follows. Section II collects the required definitions and notations from the relevant literature. In Section III, we state the problem of interest and review a framework for nonlinear kernel analysis given in [6] to present the proposed experimental setting. This builds on the results for the linear controller case [4] and leads to the development of the proposed validation tests of Section IV from [6]. A case study for a dynamic mass system followed by a more practical biomedical engineering example of blood pressure control in Section V reveals the versatility and applicability of the proposed tests. Section VI contains concluding remarks and future research directions.

II. Preliminaries

We shall denote $\mathscr{L}_2^m[0,\infty)$ (in short $\mathscr{L}_2^m$ or $\mathscr{L}_2$) a vector space of $\mathbb{R}^m$ valued square integrable functions with norm defined by $\|f\| := (\int_0^\infty f^T f\ dt)^{1/2}$. Let $\mathcal{T}_T$ be a truncation operator on the vector space of functions mapping from $\mathbb{R}$ to $\mathbb{R}^m$ by $\mathcal{T}_T f(t) = f(t)$ if $t \le T$, $\mathcal{T}_T f(t) = 0$ if $t > T$. Let $\mathscr{L}_{2e}^m[0,\infty)$ (in short $\mathscr{L}_{2e}^m$ or $\mathscr{L}_{2e}$) denote the extended space of functions $f : \mathbb{R} \to \mathbb{R}^m$ satisfying $\mathcal{T}_T f \in \mathscr{L}_2,\ \forall T > 0$. In contrast, let $\mathscr{H}_2$ be a vector space of matrix-valued functions $F(s)$ analytic in the open right-half plane such that $\|F\| := \sup_{\sigma>0}(\frac{1}{2\pi}\int_\infty^\infty |F(\sigma + j\omega)|^2\ d\omega)^{1/2} < \infty$. Also, let $\mathscr{H}_\infty$ denote the space of bounded functions in the open right-half plane such that $\|F\|_\infty := \sup_{\omega\in\mathbb{R}} \bar{\sigma}[F(j\omega)] < \infty$, where $\bar{\sigma}(F)$ denotes the largest singular value of $F(s)$. We shall denote the real rational subspace of $\mathscr{H}_2$ (resp. $\mathscr{H}_\infty$) by $\mathscr{RH}_2$ (resp. $\mathscr{RH}_\infty$). As $\mathscr{L}_2$ and $\mathscr{H}_2$ form an isomorphism via the

The authors are all with the Department of Information Engineering, Research School of Information Sciences and Engineering, The Australian National University, Canberra ACT 0200, Australia.

Brian D. O. Anderson is also with National ICT Australia Ltd., Locked Bag 8001, Canberra, ACT 2601, Australia.

Corresponding Author: Sung H. Cha.

978-89-956056-9-1/09/©2009 ACA

Laplace transform (the Parseval's relations), $f(t) \in \mathscr{L}_2$ and $F(s) \in \mathscr{H}_2$ will be used interchangeably.

Definition 1: The operator $\Sigma^x : \mathscr{L}_{2e}^m \to \mathscr{L}_{2e}^k$ with an initial condition $x \in \mathcal{X}_\Sigma \subset \mathbb{R}^n$ is said to be ***causal*** if $\Sigma^x(f) \in \mathscr{L}_{2e}^k$ is uniquely determined for $\forall f \in \mathscr{L}_{2e}^m$ and $\forall x \in \mathcal{X}_\Sigma$, and $\mathcal{T}_T\Sigma^x\mathcal{T}_T = \mathcal{T}_T\Sigma^x$ holds for $\forall T > 0$ and $\forall x \in \mathcal{X}_\Sigma$.

Definition 2: The operator is said to be ***bounded*** if it is causal and there exists a finite constant γ and a scalar function ϕ with $\phi(0) = 0$ such that $\|\Sigma^x(u)\|_2 \le \gamma\|u\|_2 + \phi(x), \forall u \in \mathscr{L}_2^m, \forall x \in \mathcal{X}_\Sigma$. The minimum value of γ which satisfies this inequality is called the gain, denoted by $\|\Sigma\|_{2_i}$.

Definition 3: The operator is said to be ***weakly Lipschitz*** (or weakly Lipschitz continuous) if it is causal and its Lipschitz semi-norm

$$\|\mathcal{T}_T\Sigma^x\|_L := \sup_{\substack{u,\nu \in \mathscr{L}_{2e}^m \\ \mathcal{T}_T u \neq \mathcal{T}_T \nu}} \frac{\|\mathcal{T}_T\Sigma^x u - \mathcal{T}_T\Sigma^x \nu\|}{\|\mathcal{T}_T u - \mathcal{T}_T \nu\|} \qquad (1)$$

is finite for every $T > 0$ and $x \in \mathcal{X}_\Sigma$.

Definition 4: The operator Σ^x is said to be ***smoothing*** if it is weakly Lipschitz and for every $T > 0$, $\gamma > 0$ and $x \in \mathcal{X}_\Sigma$ there exists $t_1 = t_1(T, \gamma, x) \in (0, T)$ such that

$$\|\mathcal{T}_{t+t_1}(\Sigma^x\mathcal{T}_{t+t_1} - \Sigma^x\mathcal{T}_t)\|_L \le \gamma \qquad (2)$$

holds for $\forall t \in [0, T - t_1]$.

Definition 5: The operator $\Sigma_w^x : \mathscr{L}_{2e}^m \Rightarrow \mathscr{L}_{2e}^k$ is said to be ***parameterized*** with $w \in \mathscr{L}_{2e}^l$ if there exists an associated operator $\Sigma^x : \mathscr{L}_{2e}^{(l+m)} \Rightarrow \mathscr{L}_{2e}^k$ such that $\Sigma_w^x(u) = \Sigma^x(w, u), \forall u \in \mathscr{L}_{2e}^m, \forall w \in \mathscr{L}_{2e}^l, \forall x \in \mathcal{X}_{\Sigma_w}$. A parameterized operator Σ_w^x is said to be ***parametrically linearly bounded*** if there exists a finite constant γ and a scalar function ϕ with $\phi(0) = 0$ such that $\|\Sigma_w^x(u)\|_2 \le \gamma\|(w, u)\|_2 + \phi(x) \quad \forall u \in \mathscr{L}_{2e}^m \quad \forall w \in \mathscr{L}_{2e}^l \quad \forall x \in \mathcal{X}_\Sigma$. The minimum value of γ which satisfies this inequality is called the parametric gain and denoted by $\|\Sigma_w\|_{p_i}$.

A. Kernel representations

Since a nonlinear left fractional representation is absent in most cases, we utilize *kernel representations* from [5].

Definition 6: Consider a causal operator $P : \mathscr{L}_{2e}^m \to \mathscr{L}_{2e}^k$ with an initial condition space $\mathcal{X}_P$. Then a causal operator $R_P^{x_P} : \mathscr{L}_{2e}^m \times \mathscr{L}_{2e}^k \to \mathscr{L}_{2e}^k, \ \forall x_P \in \mathcal{X}_P$ is called a ***kernel representation*** of P if for $\forall x_P \in \mathcal{X}_P$ and $\forall u \in \mathscr{L}_{2e}^m$, $y = P^{x_P}u \Leftrightarrow R_P^{x_P}(u, y) = 0$ holds with $y \in \mathscr{L}_{2e}^k$.

Definition 7: A kernel operator $R_P^{x_P}$ is ***well-defined*** if there exists the causal operator $(R_P^{x_P})^\# : \mathscr{L}_{2e}^m \times \mathscr{L}_{2e}^k \to \mathscr{L}_{2e}^k$ such that $y = (R_P^{x_P})^\#(u, z) \Leftrightarrow R_P^{x_P}(u, y) = z, \forall x_P \in \mathcal{X}_P$, $\forall u \in \mathscr{L}_{2e}^m$ and $y, z \in \mathscr{L}_{2e}^k$.

We assume that all kernel representations are well-defined.

Definition 8: A bounded operator $R_\Sigma^{x_P} : \mathscr{L}_{2e}^{(m+k)} \to \mathscr{L}_{2e}^k$ is ***coprime*** if there exists a bounded operator $M^{x_P} : \mathscr{L}_{2e}^k \to \mathscr{L}_{2e}^{(m+k)}$ such that $R_\Sigma^{x_P} M^{x_P} = I$ for all $x_P \in \mathcal{X}_\Sigma$.

The feedback configuration $[P, C]$ in the kernel representation is shown in Fig. 1.

Definition 9: Consider $P : \mathscr{L}_{2e}^m \to \mathscr{L}_{2e}^k$ with $\mathcal{X}_P$ and $C : \mathscr{L}_{2e}^k \to \mathscr{L}_{2e}^m$ with $\mathcal{X}_C$. Suppose we have kernel representations of P and C as $R_P : \mathscr{L}_{2e}^{(m+k)} \to \mathscr{L}_{2e}^k$ and $R_C : \mathscr{L}_{2e}^{(k+m)} \to \mathscr{L}_{2e}^m$, respectively. If R_P and R_C are interconnected to form a feedback loop as shown in Fig. 1, then a ***closed-loop kernel representation*** $R_{[P,C]} : \mathscr{L}_{2e}^{(m+k)} \to \mathscr{L}_{2e}^{(k+m)}$ is defined as

$$(z_P, z_C) := R_{[P,C]}^{(x_p, x_c)}(u, y) = \begin{pmatrix} R_P(u, y) \\ R_C(y, u) \end{pmatrix}, \qquad (3)$$

for $\forall (x_P, x_C) \in \mathcal{X}_{PC}$, where $\mathcal{X}_{PC} := \mathcal{X}_P \times \mathcal{X}_C$.

Definition 10: $[P, C]$ with a weakly Lipschitz kernel representation $R_{[P,C]} : (u, y) \mapsto (z_P, z_C)$ of Fig. 1 is ***null well-posed*** if $\forall (x_P, x_C) \in \mathcal{X}_{PC}$, $R_{[P,C]}^{-1} : (z_P, z_C) \mapsto (u, y)$ exists and it is weakly Lipschitz. Also, $[P, C]$ is ***null internally stable*** if it is null well-posed and $R_{[P,C]}^{-1}$ is bounded.

B. A modified version of Small Gain Theorem

We shall modify the original small gain theorem given in [9] to deal with $[P, C_d]$, where C_d is a parameterized operator, as shown in Fig. 2.

Theorem 11: Consider the system depicted in Fig. 2 with an operator $P : \mathscr{L}_{2e}^m \to \mathscr{L}_{2e}^k$ and a parameterized operator $C_d : \mathscr{L}_{2e}^k \to \mathscr{L}_{2e}^m$ with $d \in \mathscr{L}_{2e}$. Let us define $w := u - C_d(e)$ and $r := e - P(u)$, where $e := (y + r)$. Suppose P is bounded and C_d is parametrically linearly bounded. If $\|P\|_{p_i}\|C_d\|_{p_i} < 1$, then the mapping $H_d : \binom{r}{w} \mapsto \binom{y}{u}$ is parametrically linearly bounded.

Proof: The proof is very similar to the original proof in [9], but one requires to use the notion of parameterically linearly boundedness in Definition 5 for C_d, instead. ■

III. Problem Set-up and Analysis Results

The considered problem can be described as follows: Given an unknown plant P, which is stabilized by a known controller C_0 in a feedback setting, how can one verify if the introduction of the new controller C_1 will stabilize the unknown P *a priori*?

For the LTI systems, a complete solution to this problem can be found in [4]. Our earlier research in [6] extends the LTI analysis results in [4] for nonlinear systems using kernel representations as a generalization of left factorizations.

Lemma 12: Let R_P, R_{C_I} and R_{C_J} be bounded and weakly Lipschitz kernel representations for the operators P, C_I and C_J, respectively. Suppose $R_{[P,C_I]}$ and $R_{[P,C_J]}$ are kernel representations of $[P, C_I]$ and $[P, C_J]$, respectively. Suppose $[P, C_I]$ is null internally stable; then one can define

$$Q_{C_I}^{C_J} : \mathcal{Z}_{PC_I} \to \mathcal{Z}_{PC_J} := R_{[P,C_J]}^{x_{PC_J}} \circ [R_{[P,C_I]}^{x_{PC_I}}]^{-1}, \qquad (4)$$

where $Q_{C_I}^{C_J}(z_P, z_{C_I}) = ([Q_{C_I}^{C_J}]_1(z_P, z_{C_I}), [Q_{C_I}^{C_J}]_2(z_P, z_{C_I}))$, and there holds $[Q_{C_I}^{C_J}]_1(z_P, z_{C_I}) = z_P \in \mathcal{Z}_P$.

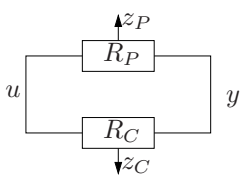

Fig. 1. Kernel configuration $[P, C]$.

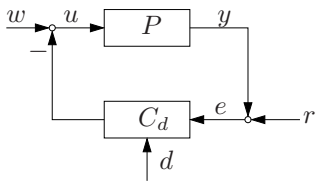

Fig. 2. Modified feedback setting.

Proof: See [6] for the details of proof. ■

Lemma 13: The projection, Proj : $\mathscr{L}_{2e}^{(m+k)} \to \mathscr{L}_{2e}^{m}$, defined as Proj$(a,b)=a$, is weakly Lipschitz and bounded.

Proof: The proof is trivial. ■

Now, we shall construct an experimental setting for the nonlinear case. Let R_P and R_{C_0} be the kernel representations of P and C_0, respectively, where $R_P(u,y)=w$ and $R_{C_0}(y,u)=r$. If we assume that $[P,C_0]$ is null internally stable, we have a bounded operator, $R_{[P,C_0]}^{-1}:(w,r)\mapsto(u,y)$. We add $R_{C_1}:(y,u)\mapsto z$, the kernel operator of C_1, to $R_{[P,C_0]}^{-1}$ as shown in Fig. 3.

Theorem 14: [6] Let R_P, R_{C_0} and R_{C_1} be bounded and weakly Lipschitz kernel representations for the operators P, C_0 and C_1, respectively. Suppose $R_{[P,C_0]}$ and $R_{[P,C_1]}$ are kernel representations of $[P,C_0]$ and $[P,C_1]$, respectively, and assume $[P,C_0]$ is null internally stable (ie. $[R_{[P,C_0]}^{x_{PC_0}}]^{-1}$ exists, is weakly Lipschitz and bounded). Then one can define a family of mappings $T_w : r\in\mathcal{Z}_{C_0}\mapsto z\in\mathcal{Z}_{C_1}$ parameterized by w

$$T_w(r) := R_{C_1}^{x_{C_1}} \circ [R_{[P,C_0]}^{x_{PC_0}}]^{-1}(w,r) \tag{5}$$

as shown in Fig. 3. Here, the following are equivalent:

(a) $[P,C_1]$ is null internally stable;
(b) $T_w^{-1}: z\in\mathcal{Z}_{C_1}\mapsto r\in\mathcal{Z}_{C_0}$ exists, is weakly Lipschitz and parametrically bounded.

Proof: See [6] for the details of proof. ■

We still want to verify the internal stability of closed-loop system $[P,C_1]$ *a priori* given C_0 and C_1 are known, and a *limited* data collected from $[P,C_0]$, where P is unknown, which is discussed in the next section.

IV. Proposed Data-based Stability Tests

For the LTI case, [4] provides two data-based stability tests, but it is not straightforward to extend for the nonlinear cases. Even if our analysis results in [6] can be applied for the nonlinear plant and/or controllers, the nonlinear version of the stability test in [6] requires the following reformulation of our problem of interest. Let us assume that C_1 is nonlinear and has a particular structure as $C_1=C_1^L+C_1^{NL}$, where C_1^L denotes the linear part and C_1^{NL} denotes the nonlinear part. Yet, $[P,C_0]$ is assumed to be stable, where the components P and C_0 are LTI. For this newly formulated problem, we will treat C_1 by combining the existing LTI tests from [4] with an additional test using the small gain theorem.

Let $\mathbf{C}_0=\tilde{V}_0^{-1}\tilde{U}_0$ be a left coprime factorization over $\mathscr{RH}_\infty$. Since we assume that $C_1=C_1^L+C_1^{NL}$, one can express the LTI part, $\mathbf{C}_1^L$, using a left coprime factorization over $\mathscr{RH}_\infty$ as $\mathbf{C}_1^L:=(\tilde{V}_1^L)^{-1}\tilde{U}_1^L$. Since we have

$$C_1=(\tilde{V}_1^L)^{-1}\tilde{U}_1^L+C_1^{NL}=(\tilde{V}_1^L)^{-1}(\tilde{U}_1^L+\tilde{V}_1^L C_1^{NL}), \tag{6}$$

by Definition 6 a kernel operator for C_1 can be expressed as

$$R_{C_1}(y,u)=[-(\tilde{U}_1^L+\tilde{V}_1^L C_1^{NL}) \quad \tilde{V}_1^L]\begin{pmatrix}y\\u\end{pmatrix}. \tag{7}$$

Furthermore, we separate this into $R_{C_1}=R_{C_1}^L+R_{C_1}^{NL}$, where

$$R_{C_1}^L(y,u) := [-\tilde{U}_1^L \ \tilde{V}_1^L]\begin{pmatrix}y\\u\end{pmatrix} \tag{8}$$

$$R_{C_1}^{NL}(y,u) := -\tilde{V}_1^L C_1^{NL}(y). \tag{9}$$

One can build an experiment setting as shown in Fig. 4.

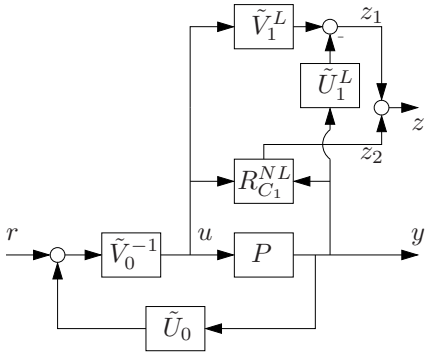

Fig. 4. Nonlinear experiment setting.

From Fig. 4, we define $T_w : r\mapsto z$ as in (5)

$$\begin{aligned} z &= T_w(r) = R_{C_1}\circ R_{[P,C_0]}^{-1}(w,r)\\ &= [-\tilde{U}_1^L \ \ \tilde{V}_1^L]\circ R_{[P,C_0]}^{-1}(w,r) + R_{C_1}^{NL}\circ R_{[P,C_0]}^{-1}(w,r)\\ &= (T_w^L+T_w^{NL})r \end{aligned} \tag{10}$$

where $z_1 := T_w^L(r)=[-\tilde{U}_1^L \ \ \tilde{V}_1^L]\circ R_{[P,C_0]}^{-1}(w,r)$ and $z_2 := T_w^{NL}(r)=R_{C_1}^{NL}\circ R_{[P,C_0]}^{-1}(w,r)$ providing $z=z_1+z_2$. We shall now use the small gain theorem, discussed in Section II-B, to verify the internal stability of $[P,C_1]$.

Theorem 15: [6] Let $[P,C_0]$ be null internally stable. Let $C_0=\tilde{V}_0^{-1}\tilde{U}_0$ be a left coprime factorization over $\mathscr{RH}_\infty$. Suppose $C_1=C_1^L+C_1^{NL}$, where the LTI part, $C_1^L=(\tilde{V}_1^L)^{-1}\tilde{U}_1^L$, is a left coprime factorization over $\mathscr{RH}_\infty$ and the nonlinear part, C_1^{NL}, has a kernel representation $R_{C_1}^{NL}$ as (9). Suppose $R_{[P,C_0]}$ and $R_{[P,C_1^L]}$ are kernel representations of $[P,C_0]$ and $[P,C_1^L]$, respectively. Consider the configuration in Fig. 4 and define the mappings $T_w^L : r\mapsto z_1$ and $T_w^{NL} : r\mapsto z_2$ to be as in (10). Given the following conditions:

(a) $[P,C_1^L]$ is internally stable;
(b) $R_{C_1}^{NL}$ is smoothing;
(c) T_w^{NL} is parametrically linearly bounded;
(d) $\|T_w^{NL}\|_{2_i}\|(T_0^L)^{-1}\|_{2_i}<1$,

we conclude $[P,C_1]$ is null internally stable.

Proof: See [6] for the details of proof. ■

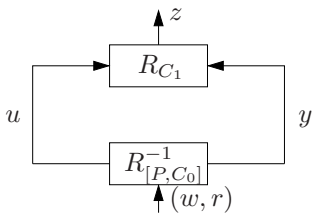

Fig. 3. Experiment setting for Kernel Representation.

V. Numerical Examples

A. Simple dynamic mass system

Consider a LTI mass system P consist of two (internal) states $x = [x_1 \quad x_2]$, one being the position and the other being the velocity of a mass in [m] and [m/s], respectively. Suppose the mass is 1 [kg] and the input u is a control force in [N] driving the velocity of the mass. The dynamics of P are given as

$$\dot{x}(t) = Ax(t) + Bu(t); \quad y(t) = Cx(t),$$

where $A = \left[\begin{smallmatrix} 0 & 1 \\ 0 & 0 \end{smallmatrix}\right]$, $B = [0 \ 1]'$ and $C = \left[\begin{smallmatrix} 1 & 0 \\ 0 & 1 \end{smallmatrix}\right]$ with full state measurements available. For this P, [7] designs a nonlinear state feedback regulator to drive the system from its initial condition to the zero state with two constraints on position of the mass, $0 \le x_1(t) \le 1$, and control input, $|u(t)| < 10$.

Our proposed test in Theorem 15 assumes that the plant P is operating with a pre-designed LTI controller C_0 where $[P, C_0]$ is (null) internally stable. Let C_0 be

$$\mathbf{C}_0(s) = \left[\ \tfrac{-6s-24}{s^2+10s+21} \ \ \tfrac{-14s-44}{s^2+10s+21} \ \right]',$$

with a left coprime factorization $C_0 = \tilde{V}_0^{-1}\tilde{U}_0$, where

$$\tilde{V}_0(s) = \frac{s+7}{s+4}, \quad \tilde{U}_0(s) = \left[\ \tfrac{-6s-24}{s^2+7s+12} \ \ \tfrac{-14s-44}{s^2+7s+12} \ \right]'.$$

Suppose the use of C_1 become attractive in the light of a crude estimate of P obtained using data from $[P, C_0]$. We test the nonlinear C_1 given in [7], which is designed to have a stable closed-loop, using our proposed results. One should notice that our proposed test in Theorem 15 requires the controller to be tested in the form of $C_1 = C_1^L + C_1^{NL}$, where C_1^L is the linear part and C_1^{NL} is the nonlinear part of controller C_1. However, the controller in [7] is given as a nonlinear control law of the form $u(x) := Kx + u_{NL}(x)$, where K is a 1×2 matrix to form the linear part and $u_{NL}(x)$ is a nonlinear function of the internal state $x(t)$. Hence, we need to implement the given state feedback law $u(x)$ not as a state feedback, but as an output feedback system with a standard state estimator. In particular, we shall implement the linear part of the state feedback law, $u_L(x) = Kx$ as C_1^L, and the nonlinear part, $u_{NL}(x)$ as C_1^{NL}.

Furthermore, as the left coprime factors of the linear part C_1^L are required, we utilize a specific state estimation/feedback controller structure, given in [10], which separates the controller into the feed-forward part and feedback part as shown in Fig. 5.

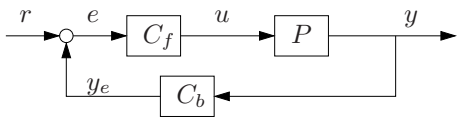

Fig. 5. State estimation/feedback implementation for C_1^L.

For the plant P, the feed-forward compensator is given as

$$C_f(s) := K(sI - A - K_eC - BK)^{-1}B \ + \ I \qquad (11)$$

and the feedback compensator is given as

$$C_b(s) := K(sI - A - K_eC)(-K_e), \qquad (12)$$

where K is the given (linear) feedback gain (ie. $u(x) = Kx$), K_e is the estimator gain. For the nonlinear part, we implement C_1^{NL} by utilizing the same estimator gain K_e used for the linear part as shown in Fig. 6.

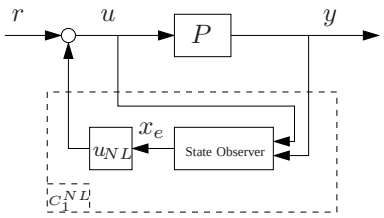

Fig. 6. State estimation/feedback implementation for C_1^{NL}.

Also, [10] provides the basis for an implementation of C_1^{NL} as a state-space realization

$$\begin{aligned} \dot{x}_e &= (A + K_eC + BK)x_e + Br - K_ey; \\ u &= u_{NL}(x_e) + r. \end{aligned} \qquad (13)$$

Let x_f and x_b be internal states of $C_f(s)$ and $C_b(s)$, respectively. From Fig. 5, $C_f(s)$ can be implemented as a state-space realization

$$\dot{x}_f = (A+K_eC+BK)x_f+B(r+y_e); \quad u = Kx_f+e \ (14)$$

and $C_b(s)$ can be similarly implemented as

$$\dot{x}_b = (A + K_eC)x_b - K_ey; \quad y_e = Kx_b. \qquad (15)$$

If we add (14) and (15),

$$\dot{x}_f + \dot{x}_b = (A + K_eC + BK)(x_f + x_b) + Br - K_ey,$$

which is exactly the standard state estimator given in (13) with $x_e := x_f + x_b$.

Given $K = [-116.53 \ \ -28.232]$, the linear part of the state feedback law $u = Kx$ can be implemented as

$$\mathbf{C}_1^L(s) = \left[\ \tfrac{-349.6s-1398}{s^2+35.23s+96.7} \ \ \tfrac{-229.5s-804.9}{s^2+35.23s+96.7} \ \right]',$$

with a left coprime factorization $C_1^L = (\tilde{V}^L)_1^{-1}\tilde{U}_1$, where

$$\tilde{V}_1^L(s) = \frac{s+32.23}{s+4}, \ \tilde{U}_1^L(s) = \left[\ \tfrac{-349.6s-1398}{s^2+7s+12} \ \ \tfrac{-229.5s-804.9}{s^2+7s+12} \ \right]'.$$

The nonlinear part of the state feedback law is given as

$$\begin{aligned} u_{NL}(x) &= 43.859x_1^2 - 3.2071x_1x_2 - 27x_2^2 + 39.006x_1^3 \\ &+ 19.394x_1^2x_2 + 8.3457x_1x_2^2 - 21.397x_2^3 + 26.547x_1^4 \\ &+ 13.825x_1^3x_2 + 12.307x_1^2x_2^2 + 6.0256x_1x_2^3 - 7.2784x_2^4 \\ &- 1.1292x_1^5 - 1.6559x_1^4x_2 + 7.6888x_1^3x_2^2 + 6.8941x_1^2x_2^3 \\ &+ 2.6510x_1x_2^4 - 0.76859x_2^5, \end{aligned} \qquad (16)$$

where $x = (x_1, x_2)$ is the system state.

Following the validation test proposed in Theorem 15, we are first required to validate $[P, C_1^L] \in \mathscr{RH}_\infty$. To do that, we set up the experiment configuration of Fig. 4 and utilize the necessary and sufficient test given in [4, Theorem 11].

The simulation indicates that $|T_0^L - 1| \leq 1,\ \forall \omega \geq \omega_0 = 4.5$ rad/s as shown in Fig. 7. One can then see in Fig. 8 that unwarg $T_0^L(j0) = 0$ and unwarg $T_0^L(j\omega_0) = -0.278\pi$, which satisfies the conditions and hence $[P, C_1^L] \in \mathscr{RH}_\infty$.

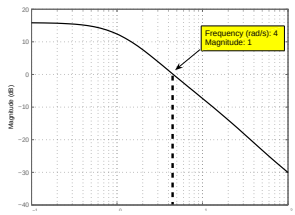

Fig. 7. Magnitude of $T_0^L - 1$

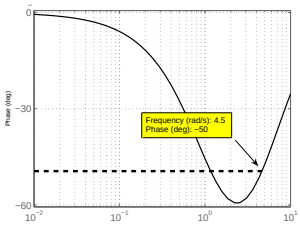

Fig. 8. Phase of T_0^L

Now we need to check the smoothing condition of $R_{C_1}^{NL}$. From (9), we know that $R_{C_1}^{NL}$ is simply a cascade of two operators. Simulation results reveal that C_1^{NL} is smoothing as long as the state, $x = [x_1 \ \ x_2]$, is confined over a bounded subset of $\mathcal{X}_P$. In fact, one can show that $R_{C_1}^{NL}$ is smoothing because $\tilde{V}_1^L$ is linear and C_1^{NL} is smoothing. Consider the configuration in Fig. 4. Simulation also reveals that T_w^{NL} is parametrically linearly bounded as C_1^{NL} is bounded for bounded states x_1 and x_2. We determined an upper bound of $\|T_w^{NL}\|_{2_i}$ as 0.01 using

$$\|T_w^{NL}\|_{2_i} \leq \|\tilde{V}_1^L\|_{2_i} \|C_1^{NL}\|_{2_i} \|R_{[P,C_0]}^{-1}\|_{2_i}. \qquad (17)$$

Here, the exact value of $\|\tilde{V}_1^L\|_{2_i}$ can be computed numerically as $\tilde{V}_1^L$ is known and an upper bound of $\|C_1^{NL}\|_{2_i}$ can be given from the controller design stage. Furthermore, an upper bound of $\|R_{[P,C_0]}^{-1}\|_{2_i}$ can be determined experimentally. Note that $[P, C_1^L]$ is internally stable according to the aforementioned discussion and we can calculate $\|(T_0^L)^{-1}\|_{2_i}$, which is found to be 7.2307. This implies $\|T_w^{NL}\|_{2_i}\|(T_0^L)^{-1}\|_{2_i} \leq 0.0723 < 1$ and an experiment reveals that $[P, C_1]$ is internally stable.

B. Blood Pressure control system

A major side effect of cardiac surgery is that patients can become hypertensive, requiring treatment to prevent cardiac dysfunction, swelling and/or fluid accumulation in the lungs, reduced blood supply to the heart muscle, stroke, and bleeding. Although drugs are available for treating post-operative hypertension, gradually adjusting the dose of a medication until the desired effect is achieved in order for these drugs to regulate blood pressure is often difficult. Under-dosing leaves the patient hypertensive, whereas over-dosing can reduce the blood pressure to levels associated with shock. There has been interest in developing controllers for administering Sodium Nitroprusside (SNP), a commonly used and potent antihypertensive. Inter-patient variability as well as a patient's sensitivity to drugs motivates the use the of multiple model adaptive controllers and requires a careful design of controllers. An early example of such design is presented in [8]. Patients are modelled as open-loop stable $P(s) := e^{-Ts}\bar{P}(s)$, where $\bar{P}$ is the (undelayed) linear part and T is the infusion delay in seconds. Since the plant P is open-loop stable, a Smith predictor (SP) is used to compensate for the effect of T. We use $[P, C_i \boxplus SP]$ to denote the feedback interconnection of P and controller C_i with a built-in SP as shown in Fig. 9. Here, each C_i is designed using $\bar{P}(s)$, instead of $P(s)$. If T can be determined exactly then the closed-loop output from $[P, C_i \boxplus SP]$ will be expressed as $y_i(t) = \bar{y}_i(t-T)$, where $\bar{y}_i$ denotes the closed-loop output from $[\bar{P}, C_i]$. For the application of our nonlinear stability results of preceding sections, we set $T = 50$s and assume that this value can be measured exactly. We borrow the patient model $P(s) := e^{-Ts}\bar{P}(s)$ from [8], where

$$\bar{P}(s) := \frac{G(\tau_3 s + 1)}{[(\tau_3 s + 1)(\tau_2 s + 1) - \alpha](\tau_1 s + 1)}. \qquad (18)$$

Here, $\alpha = 0.5$ denotes the fraction of the drug recirculated and $\tau_1 = 50s, \tau_2 = 10s$ and $\tau_3 = 30s$ denote time constants associated with drug action, flow through pulmonary circulation and flow through systemic circulation, respectively. The output y is the difference between the current arterial pressure p and the initial pressure p_0 (ie. $y(t) = p_0 - p(t)$), and the plant input u is the infusion rate of drug into the patient. The only variable parameter in (18) is plant gain G in mmHg/(ml/h). In practice, the control system is expected to maintain certain performance criteria (eg. 20% settling time to be less than 10min; maximum overshoot to be less than 10mmHg with a steady-state error within 5 mmHg).

Consider $P(s)$ with $G = 0.25$ (the minimum plant gain used in [8]). Suppose a stabilizing controller C_0 is initially in the closed-loop

$$\mathbf{C}_0(s) := \frac{-196.2s^2 - 25.72s - 0.4359}{s^3 + 1.695s^2 + 0.7942s + 0.00207},$$

which has a left coprime factorization $C_0 = \tilde{V}_0^{-1}\tilde{U}_0$, where

$$\tilde{V}_0(s) = \frac{s^3 + 1.695s^2 + 0.7942s + 0.00207}{s^3 + 196.4s^2 + 25.73s + 0.4359},$$
$$\tilde{U}_0(s) = \frac{-196.2s^2 - 25.72s - 0.4359}{s^3 + 196.4s^2 + 25.73s + 0.4359},$$

with the SP built into the closed-loop as in Fig. 9. This particular controller C_0 achieves a rise-time of 60s with 6% overshoot, 63s of 20% settling time and 0.5% steady-state error, which meets the above-mentioned required performance criteria under a normal medical practice.

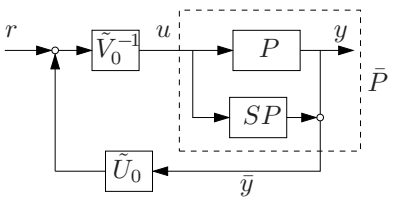

Fig. 9. Simplified initial BP control system, $[P, C_0 \boxplus SP]$.

Now, suppose the condition of patient has changed and, in turn, caused a change of G in (18) from 0.25 to 2. In this case, the controller C_0 cannot maintain the required performance specification and results in very large overshoot

(65%). Thus, C_0 has to be replaced by a better performing controller C_1. Based on measurements with $[P, C_0 \boxplus SP]$, we detect same level of gain change and using the new estimate of P, we design $C_1 := C_1^L + C_1^{NL}$, with linear part C_1^L and a nonlinear part C_1^{NL}. The linear part is

$$\mathbf{C}_1^L(s) := \frac{-29.17s^2 - 4.714s - 0.09623}{s^3 + 1.802s^2 + 0.9647s + 0.04585}$$

with a left coprime factorization $C_1^L = (\tilde{V}^L)_1^{-1}\tilde{U}_1^L$

$$\tilde{V}_1^L(s) = \frac{s^3 + 1.802s^2 + 0.9647s + 0.04585}{s^3 + 29.36s^2 + 4.862s + 0.1066}, \quad (19)$$

$$\tilde{U}_1^L(s) = \frac{-29.17s^2 - 4.714s - 0.09623}{s^3 + 29.36s^2 + 4.862s + 0.1066}. \quad (20)$$

With a design parameter, $k \in \mathbb{R}$, the nonlinear part is

$$C_1^{NL}(r, y) := k|y(t)|[r(t) - y(t)], \quad (21)$$

where r is the reference input. We choose $k = 3.5$ to achieve a rise-time similar to that of C_0 and less than 0.5% overshoot, see Table I.

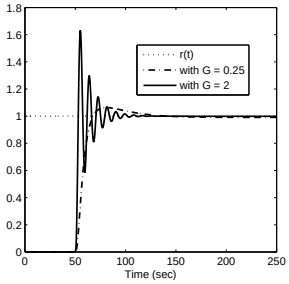

Fig. 10. $[P,C_0 \boxplus SP]$ step response

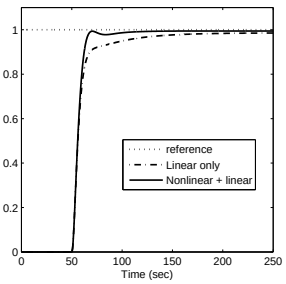

Fig. 11. $[P,C_1 \boxplus SP]$ step response

To ensure a stable closed-loop with the introduction of the new controller C_1 to the patient, we shall utilize our stability results discussed in Section IV with a slight modification as P is not LTI. As we have assumed $T = 50$s can be measured exactly, the output from $[P, C_i \boxplus SP]$, y_i, will be just a delayed version of $\bar{y}_i$ from $[\bar{P}, C_i]$. Furthermore, the mapping from u to $\bar{y}$ in Fig. 9 is, in fact, $\bar{P}$. Hence, one can conclude the internal stability of $[P, C_1 \boxplus SP]$ as long as $[\bar{P}, C_1]$ is internally stable. First, to check the internal stability of $[\bar{P}, C_1^L]$, we set up the experimental configuration from Fig. 9—similar to Fig. 4—using $\bar{y}$, instead of y. Then use the necessary and sufficient test given in [4, Theorem 11]. The simulation indicates that $|T_0^L - 1| \leq 1, \ \forall \omega \geq 10$ rad/s and unwarg $T_0^L(j0) = 0$ and unwarg $T_0^L(j\omega_0) = -0.144\pi$, which satisfies the conditions, i.e. $[P, C_1^L] \in \mathscr{H}_\infty$. Next, we shall check the smoothing property of $R_{C_1}^{NL}$. As discussed in the previous example, this is ensured by V_1^L being linear and C_1^{NL} being smoothing (via using (19) and (21) with bounded y and r). From simulations, we determine an upper bound for $\|(T_w^{NL})\|_{2_i}$ to be 0.062 using (17). Also, we can calculate $\|(T_0^L)^{-1}\|_{2_i}$, which is found to be 1. This implies $\|(T_w^{NL})\|_{2_i}\|(T_0^L)^{-1}\|_{2_i} < 1$.

The two case studies of this section show the versatility and applicability of our data-based test in real practice. For the blood pressure control, we showed how the use of a nonlinear regulator can result in a better performance.

TABLE I
CLOSED-LOOP PERFORMANCE COMPARISON

	Required	G=0.25	$G = 2$		
		C_0	C_0	C_1^L	C_1
Rise-time	<120s	60s	52.5s	66s	60.3s
Max overshoot	10_{mmHg}	6%	62%	0%	0.3%
20% Settling time	< 600s	63s	68.5s	61.5s	60s
Steady-state error	5_{mmHg}	0.5%	0%	2%	1%
Specification OK		✔	✘	✔	✔

VI. CONCLUSIONS

We have applied our test in practical control engineering problems via two particular case studies. A simple dynamic mass system was considered, where a nonlinear state feedback regulator is designed for over 40% reduction in both the rise time and settling time with zero % overshoot, compared to its linear counterpart. We also discussed how to implement the nonlinear controller given as a state feedback law for the purpose of our nonlinear controller verification. We have further considered a biomedical engineering application of blood pressure control, where a multiple-model adaptive control (MMAC) design is used for the regulation of arterial pressure. Since MMAC algorithms normally switch among several local controllers during their operation, our data-based stability verification test ensures safety, ie. preventing switching to a destabilizing controller, in this biomedical engineering application.

ACKNOWLEDGMENT

This work was supported in part by the ARC Discovery-Projects Grant DP0664427.

REFERENCES

[1] A. S. Morse, "Supervisory control of families of linear set-point controller part i. exact matching," *IEEE Transactions on Automatic Control*, vol. 41, no. 10, pp. 1413–1431, 1996.

[2] K. S. Narendra and J. Balakrishnan, "Adaptive control using multiple models," *IEEE Transsactions on Automatic Control*, vol. 42, pp. 171–187, 1997.

[3] B. D. O. Anderson and A. Dehghani, "Challenges of adaptive control–past, permanent and future," *Annual Reviews in Control*, vol. 32, pp. 123–135, 2008.

[4] A. Dehghani, B. D. O. Anderson, A. Lanzon, and A. Lecchini-Visintini, "Verifying stabilizing controllers via closed-loop noisy data: Mimo case," in *Proceedings of the 46th IEEE Conference on Decision and Control*, New Orleans, LA, USA, December 2007.

[5] A. J. Van der Schaft, *L_2-gain and passivity techniques in nonlinear control*. Berlin: Springer, 1996.

[6] S. H. Cha, A. Dehghani, and B. D. O. Anderson, "Nonlinear analysis for verifying closed-loop stability before inserting a new controller," in *Proceedings of the 2009 European Control Conference*, 2009, submitted.

[7] W. Aangenent, R. de Jong, R. van de Molengraft, and M. Steinbuch, "Time domain performance based nonlinear state feedback control of constrained linear systems," in *Proceedings of 16th IEEE International Conference on Control Applications*, 2007.

[8] J. F. Martin, A. M. Schneider, and S. N. TY, "Multiple-model adaptive control of blood pressure using sodium nitroprusside," *IEEE Transactions on Biomedical Engineering*, vol. BME-34, pp. 603–611, 1987.

[9] C. A. Desoer and M. Vidyasagar, *Feedback Systems: Input-Output Properties*. Academic Press, 1975.

[10] B. D. O. Anderson and J. B. Moore, *Optimal control: linear quadratic methods*. Englewood Cliffs, N.J.: Prentice-Hall, 1989.